Colloidal processing of chemically prepared zinc oxide varistors. Part I: Milling and dispersion of powder

Nelson S. Bell,[a] Joe Cesarano III, James A. Voigt, Steve J. Lockwood, and Duane B. Dimos
Sandia National Laboratories Albuquerque, New Mexico 87185

(Received 24 July 2003; accepted 28 October 2003)

Chemically prepared zinc oxide powders are fabricated for the production of high aspect ratio varistor components. Colloidal processing was performed to reduce agglomerates to primary particles, form a high solids loading slurry, and prevent dopant migration. The milled and dispersed powder exhibited a viscoelastic to elastic behavioral transition at a volume loading of 43–46%. The origin of this transition was studied using acoustic spectroscopy, zeta potential measurements, and oscillatory rheology. The phenomenon occurs due to a volume fraction solids dependent reduction in the zeta potential of the solid phase. It is postulated to result from divalent ion binding within the polyelectrolyte dispersant chain and was mitigated using a polyethylene glycol plasticizing additive. This allowed for increased solids loading in the slurry and a green body fabrication study to be presented in our companion paper.

I. INTRODUCTION

Colloidal processing of ceramic materials has led to the development of several novel forming methods for casting bulk ceramic pre-forms.[1] These processes can be superior to conventional forming methods when structural uniformity is a key issue and in situations where loss of material from postsintering machining and finishing processes has a significant cost impact. Often of equal importance to product quality is the negative effect that machining-induced flaws can have on performance. For example, in varistor elements, material defects or flaws (such as machining cracks or pores) severely impact electrical performance.[2] Inhomogeneities can concentrate the pulse current and nucleate high-voltage breakdown of the varistor. The purpose of the work presented here was to investigate the application of colloidal processing–based forming methods to prepare high field ZnO varistor components.

The varistor powder used in this study was prepared using an aqueous precipitation process developed at Sandia National Laboratories.[3–6] One of the challenges of developing colloidal forming processes using these powders is that their primary particles are below 200 nm in size. This small size makes them highly sinterable but complicates slurry processing. Bergstrom et al. have shown for very fine particle size powders that there is a significant effect on densification dependent on the particle interactions and formation of a homogeneous green microstructure.[7] This implies that achieving a maximum solids loading in the slurry and optimizing the formation method effects on green structure will dictate the success of part production.

Rheological characterization is commonly used to determine the maximum solids loading using the Krieger-Doughtery expression[1]

$$\eta = \eta_s \left(1 - \frac{\phi}{\phi_{max}}\right)^{-[\eta]\phi_{max}} . \quad (1)$$

In this expression, ϕ is the true volume fraction with a maximum at ϕ_{max}, η_s is the solvent viscosity and $[\eta]$ is the intrinsic viscosity, which relates to the effect on the relative viscosity of noninteracting particles in very dilute suspensions. It represents a particle shape factor beginning at 2.5 for spheres and increasing with shape anisotropy. Cube-shaped particles have a value of 4, for example.[8] A plot of the high shear rate viscosity against volume fraction can be fit with this equation to estimate the volume fraction of close-packed particles.

In this study, the processing parameters related to the formation of a colloidally stable, high solids loading suspension of the chemically prepared varistor material were investigated. The solubility of the material versus pH and the effectiveness of a polyelectrolyte dispersant were examined as solids loading was increased. The rheological characteristics of the suspension were studied and fitted with a modified Krieger–Doughtery equation to estimate the maximum packing fraction that can be achieved in the suspension. The use of processing aids such as a plasticizer were also tested.

[a]Address all correspondence to this author.
e-mail: nsbell@sandia.gov
DOI: 10.1557/JMR.2004.0179

II. EXPERIMENTAL

The composition of the chemically prepared zinc oxide is as given in Table I. These powders are produced by a two-stage aqueous coprecipitation of the chloride salts of Zn, Mn, Co, and Al.[3] Powder density was measured by helium pycnometry (VP Penta-Pyncnometer, Quantachrome Corp., Boynton Beach, FL) to be 5.58 g/cm^3.

The chemical stability of the powder was evaluated by leaching studies using ammonium hydroxide to adjust pH. Five vol% concentrations of powder were aged for 1 week under shaking, and the supernatant was characterized for each dopant by inductively coupled plasma mass spectroscopy (ICP) analysis (Elan 6000 ICP/MS, Perkin-Elmer, Shelton, CT). The uncertainty of these measurements is ±10%.

Attrition milling with 3-mm yttria-stabilized zirconia media was used to achieve a mill solid loading of 40 vol%. Ammonium polymethacrylate (PMA; Darvan C, R.T. Vanderbilt Company, Inc., Norwalk, CT) was used as dispersant at 4% to the powder dry weight. The particle size of the dispersed and milled powder was studied using dilute suspensions (<0.01 wt%) by a Coulter LS230 light scattering device (Coulter LS230, Coulter Corp., Miami, FL). Surface area was measured using the BET method (ASAP 2010, Micromeritics, Norcross, GA).

Zeta potential was measured after the addition of PMA and the milling operation using a DT 1200 acoustic spectrometer (DT1200 Acoustic Spectrometer, Dispersion Technology, Mount Kisco, NY). A concentrated suspension at pH 9 was measured for acoustic attenuation and speed of sound, conductivity, and colloid vibration impedance, and the data were used to determine particle size distribution and zeta potential. The suspension was successively diluted with deionized water preadjusted to pH 9 with ammonium hydroxide. The solid loading for each dilution was determined by weight loss. A 4.73 vol% suspension was titrated at pH 9 using 1.0 M KNO_3 solution to measure zeta potential as conductivity was increased. Similar measurements were performed on a dispersion containing 10 wt% PEG400 in the fluid phase, and a suspension at 9.8 vol% CPV powder was titrated at pH 9 with KNO_3 to compare zeta potential with monovalent salt concentration.

Rheology of the suspension was measured as a function of volume fraction using a Haake RS 300 Rheometer with a 60-mm-diameter titanium 1° cone and flat plate geometry (Haake Instruments, Paramus, NJ). The evaporation of solvent was prevented by use of a polycarbonate solvent trap and paraffin oil. Shear rates were increased from a static condition to the maximum rotation speed, held for 1 min, and decreased to the initial speed. Tests were made of the powder dispersed using PMA and following the addition of poly(ethylene glycol) 400 (PEG400) at 10% by mass of the fluid mass as a plasticizing agent.

TABLE I. Composition of zinc oxide powder.

Zinc oxide	98.94 mol%
CoO	0.25 mol%
MnO	0.25 mol%
Bi_2O_3	0.56 mol%
Al	135 ppm
Na	300 ppm

III. RESULTS

The chemical stability of the powder in an aqueous environment is important as leaching of the dopant elements to the solvent could cause changes in the electrical performance of the varistors. The surface chemistry of the synthesized powder should resemble that of bismuth oxide, as the bismuth is added after the precipitation and calcination of the doped zinc oxide powder. However, milling operations used to reduce particle size will allow the zinc and dopant elements to leach as well. Results of powder leaching at various pHs are shown in Fig. 1. Clearly, the minimum in solubility of all elements is pH 9.1. Maintaining this pH during slurry processing is important to prevent the segregation of dopants in the microstructure and avoid particle agglomeration via specific adsorption of ionic species to the particles, which reduces electrostatic stabilization.

The particle size distributions of the initial powder and after various milling times are presented in Fig. 2. The distribution of particle sizes shows that fragmentation of the initial particle agglomerates occurs and produces three distinct size fraction peaks. Long milling times did

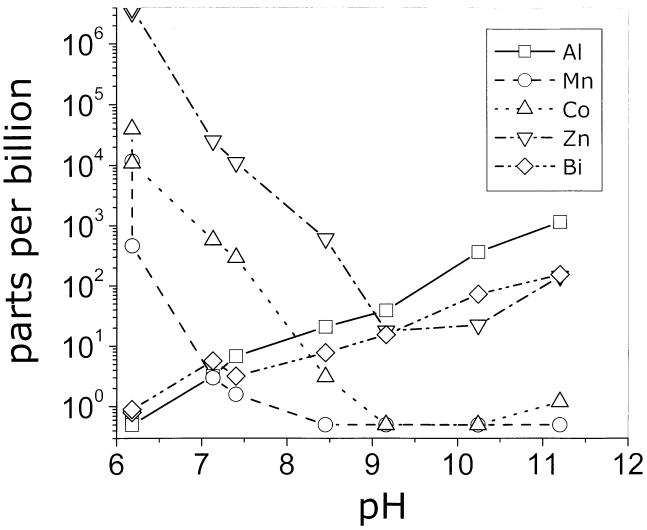

FIG. 1. Leaching of dopant and zinc ions from chemically prepared powders as a function of pH. Concentrations are measured from the supernatant of a 10 vol% suspension after agitation for 1 week. Lines are provided to guide the observer.

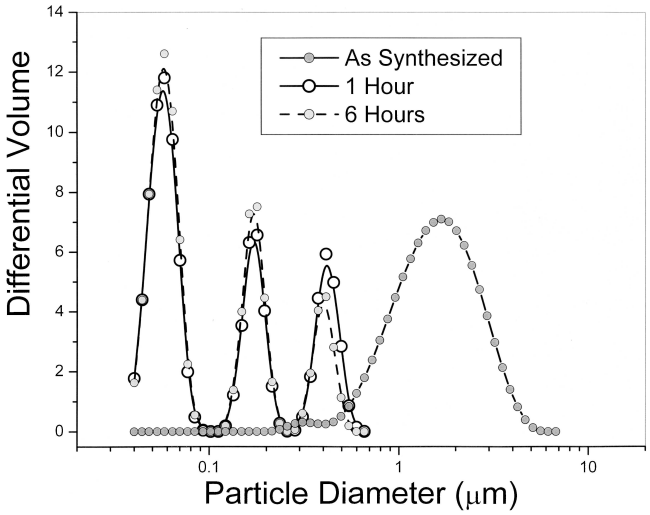

FIG. 2. Particle size distributions showing the effect of the attrition process on the initial powder distribution after 1 h of attrition milling and following 6 h of attrition milling. Lines are provided to guide the observer.

not reduce these agglomerates. Table II presents the surface area data measured using N_2 adsorption. An increase in surface area appears complete within 1 h of attrition milling.

Figure 3 shows the morphology of the synthesized powder and the morphology of particles after attrition milling and separated by sedimentation during the course of a month. The initial particles are aggregated to each other, where the agglomerates retain the morphology of the oxalate crystalline structure formed during precipitation. The apparent particle size is ultrafine and in the range of 50 nm. However, the agglomerates are "hard" with strong necks to nearest neighbors. Maximizing the solids fraction in the slurry requires milling to the primary or near primary particle size.

Figure 4(a) shows the zeta potential measured on these particles after adding 4 wt% PMA at pH 9 and the corresponding conductivity of each sample as a function of volume fraction solids in aqueous solution and a solution of 10 wt% PEG400. The PMA generates a negative zeta potential and adds a steric stabilization component from the adsorbed polymer chains.[9,10] The magnitude of the zeta potential at high solids concentration is relatively low, and the magnitude increases as solvent is added. In Fig. 4(b), the zeta potential of a 4.73 vol% suspension was measured during titration of KNO_3 electrolyte solution to characterize the screening of the PMA dispersed powder against salt addition. The zeta potential decreases in magnitude with added monovalent salt, but not as rapidly as found for the samples in Fig. 4(a). The zeta potential decreases with volume fraction more rapidly than can be attributed to the effects of electrolyte concentration alone. The addition of PEG400 inhibits the decline in zeta potential as solids loading is increased but follows the same qualitiative trend with conductance.

TABLE II. Surface area of milled powder as a function of milling time.

Milling time	Specific surface area (m^2/g)
Initial	8.66 ± 0.03
15 min	11.12 ± 0.04
30 min	11.17 ± 0.04
45 min	11.19 ± 0.05
60 min	11.15 ± 0.04

Rheological characterization was performed to determine the role of volume fraction on viscosity in the suspension and colloidal stability. Figure 5 shows the power-law relationship for volume fraction at a shear rate of 750 s^{-1}. Fits to the modified Krieger–Doughtery equation [Eq. (1)] for the effect of volume fraction on viscosity produce equation parameters of $\phi_m = 0.582$ and $[\eta] = 5.3$ for the PMA dispersed powder in water and $\phi_m = 0.63$ and $[\eta] = 4.84$ for the PMA dispersed powder with 10 wt% PEG400 added to the liquid phase.

Figure 6 shows an oscillatory stress sweep at 1 Hz for increasing volume fractions of the PMA dispersed slurry. As solids content is increased, the elastic modulus (G') becomes greater in magnitude than the loss modulus (G'') and constant over the shear stress sweep. These graphs show the development of a particle structure as volume fraction is increased. The crossover between viscoelastic and elastic behavior is frequency-dependent over the investigated solids loading. At the highest measured solids loading, elastic behavior is dominant over the entire measured range. It was not possible to characterize the exact volume fraction where a contacting particle network is formed, but estimates from our experience suggest that it ranges from 43 vol% to 46 vol% dependent on the powder lot.

IV. DISCUSSION

The solubility of dopants in the synthesized powder was evaluated first to determine the stability of the material in water. The leaching or dissolution of components mimics the expected solubility of the metal hydroxides given by hydrolysis reactions of the dopants.[11] As shown in Fig. 1, below pH values of 9, the mononuclear Zn^{2+} species was the primary solution component, and above pH 11, the $Zn(OH)_4^{2-}$ became the soluble species. Aluminum dissolves as $Al(OH)_4^-$ above pH 6. Manganese in the 2^+ state has a number of hydrolysis products that decrease in solubility as pH increases. The mononuclear species precipitate above pH 9–10 depending on solution concentration. Cobalt is stable in water in the 2^+ state, and the mononuclear species continually decreases in concentration to pH 10 where the hydroxide is stable. Bismuth rapidly becomes soluble below pH 8 due

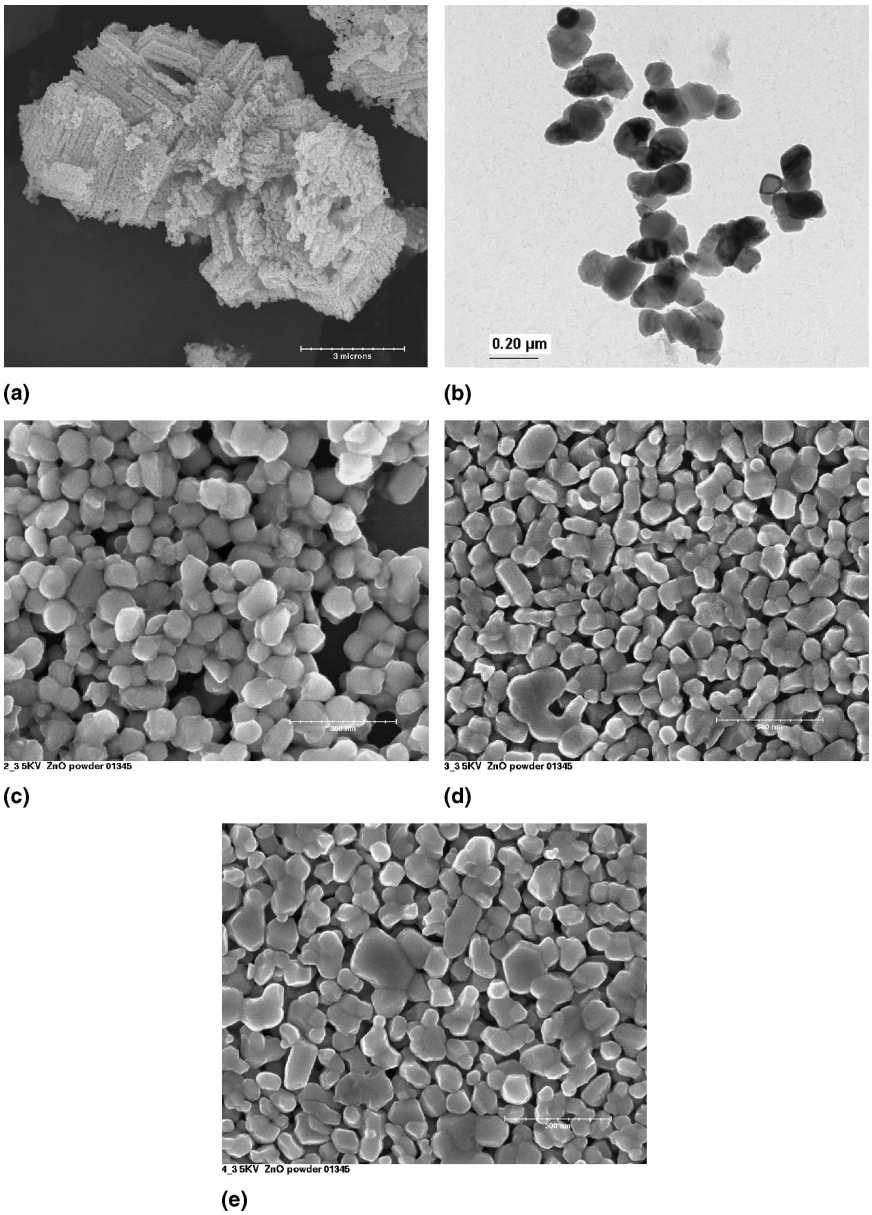

FIG. 3. Particle morphology characterization using transmission electron microscopy (TEM) and scanning electron microscopy (SEM). (a) Initial powder (SEM). The following micrographs are post attrition milling for 3 h: (b) colloidally stable nanoparticles (TEM), (c) top layer sediment (SEM), (d) mid-layer sediment (SEM), and (e) bottom layer sediment (SEM).

to the formation of polynuclear species ($Bi_9OH_{22}^{5+}$, $Bi_9OH_{21}^{6+}$), but between pH 8 and 12, the hydroxide phase is dominant. The slight rise in Bi^{3+} observed in these tests relates to the formation of $Bi(OH)_4^-$. With the exception of bismuth species, the low concentrations measured in the solution suggest that polynuclear species do not play a large role in leaching. The lowest concentration of dopants was found to be at pH 9.1. Maintaining this value of pH should enhance material stability.

The attrition milling process used in slurry preparation was functionally complete in 1 h. Table II shows the specific surface area of the powder at intervals of this first hour. Significant increases in surface area are not indicated by the data, though particle size distributions shown in Fig. 2 clearly show the breakdown of the aggregates. Maximizing a size reduction process requires consideration of particle stability, energy input, and milling time. Because attrition milling inputs a large amount of energy into grinding, it is not likely that further operations will further reduce the particle size.

It is clear that the porous aggregates are fracturing into distinct populations, which are stable against further

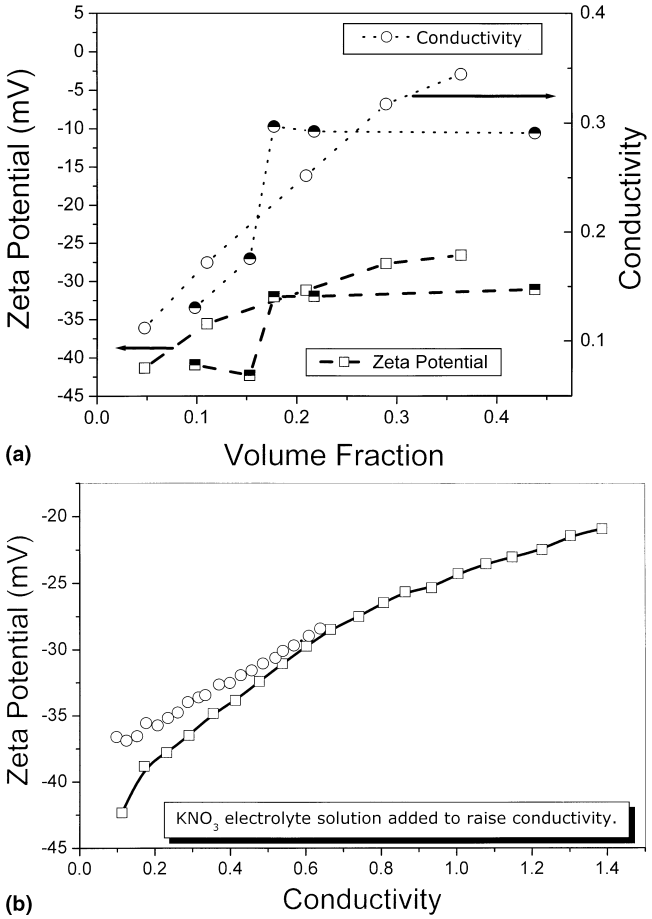

FIG. 4. (a) Zeta potential versus volume fraction of a slurry dispersed with 4 wt% Darvan C (PMA) with respect to the powder mass. Open symbols are in aqueous suspension; halftones are in 10 wt% PEG400. (b) Zeta potential as background electrolyte is increased with KNO_3. Squares are for a 4.73 vol% dispersed suspension in pH 9 water, and circles are for a 9.8 vol% dispersed suspension in 10 wt% PEG400.

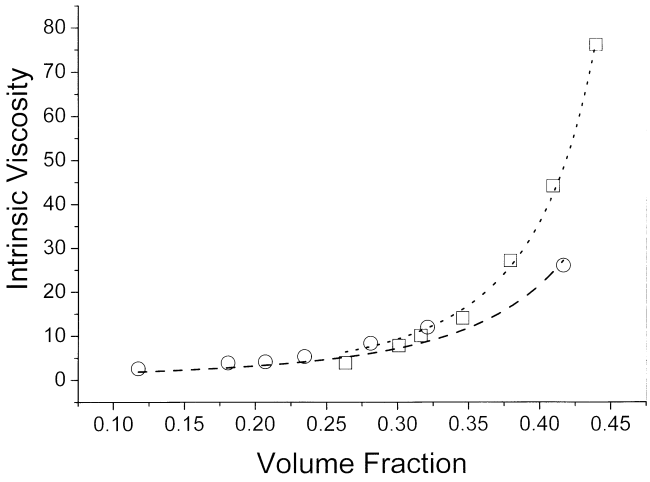

FIG. 5. Intrinsic viscosity of CPV powder dispersed with 4 wt% Darvan C in pH 9 water (squares) and in a fluid mixture of 10% PEG400–90% pH 9 water. Lines are plots of the modified Krieger–Doughtery equation with parameters $\phi_m = 0.582$, $[\eta] = 5.3$ and $\phi_m = 0.63$, $[\eta] = 4.84$.

milling. A dilute particle suspension was allowed to sediment, and particles were sampled as a function of stability and sedimentation time to examine the milled particle morphology. Scanning electron micrographs of sedimentation fractions of the milled powder cannot distinguish distinct particle size fractions shown in Fig. 3. Distinct separation of particle sizes as seen in the particle size distribution data was not possible. There is a difference in morphology of the most stable particles (smallest size) and the rapidly sedimented particle fraction (largest size). The highly stable particles are roughly equiaxed and approximately 50 nm in diameter. Their small size promotes their stability to gravimetric sedimentation, and the dispersant prevents particle agglomeration. The largest particles are sintered aggregates of submicrometer-size particles with distinct grain boundaries between the aggregates rather than the porous structure of the synthesized aggregates. The approximate size of the aggregates is 400 nm, and their arrangement is non-equiaxed. The individual grains within the large size aggregates are approximately 100–200 nm in size. Based on these observations, we propose that the as-synthesized aggregates are constructed as a surface layer of nanosize particles with a core of more strongly aggregated submicrometer-size grains. The intermediate grains between the core and exterior are larger than the nanosize fraction and lie in the range 100–200 nm. The milling process fractures the necks between crystallites to separate the nanosize and intermediate populations but does not provide enough energy to fracture the core aggregates.

The sedimented fractions of particles show color variations that suggest chemical inhomogeneity in the particle populations. The fine, nanosize particles are blue in color, the intermediate-size particles are green, and the large aggregates that settle rapidly are distinctly yellow. Bismuth oxide is yellow in color, and examination by x-ray diffraction produced peaks for bismuth oxide and zinc oxide in this sediment. The blue and green populations only provided zinc oxide peaks. Based on these observations, it appears that the fragmentation of the calcined aggregates into these populations relates to the amount of bismuth oxide precipitated in the fabrication process. We propose that the distribution of bismuth oxide is inhomogeneous within the doped zinc oxide aggregate pore structure. During milling, those particle necks with high content of bismuth oxide are too strong for the milling procedure to break down during the initial hour. They may be further reduced with additional milling time, but that raises the possibility of contamination by the milling media.

Particle dispersion was performed as a component of attrition milling. Ammonium polymethacrylate (PMA) was used to increase the zeta potential of the particles

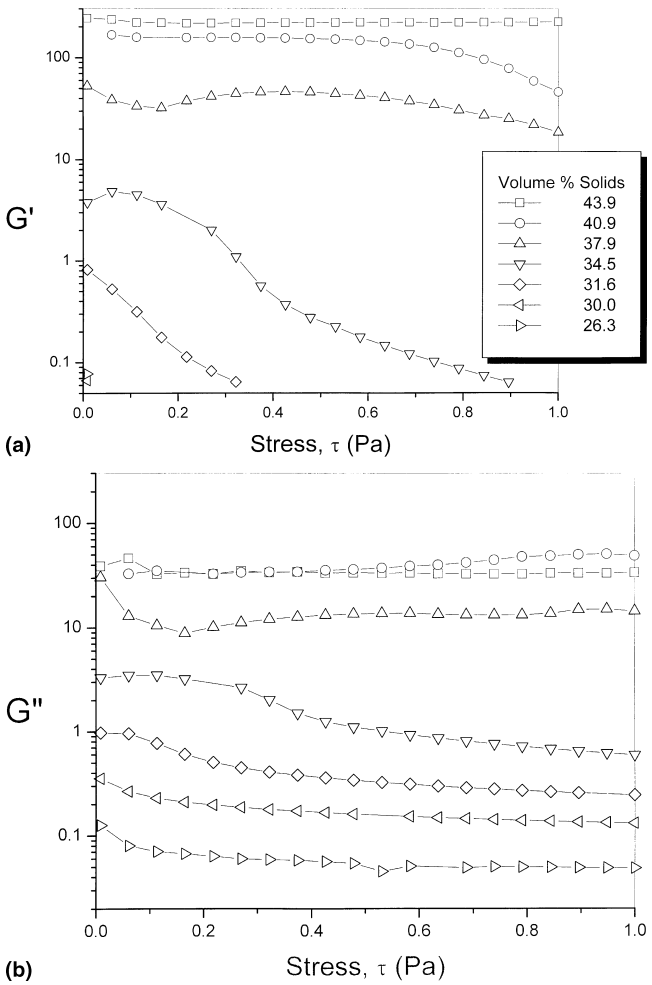

FIG. 6. Stress sweep versus ϕ for the CPV powder milled and dispersed with 4 wt% Darvan C in water. (a) Elastic modulus versus stress and (b) loss modulus versus stress.

under this pH constraint and provide a steric component to repulsion due to the adsorbed polymer chains. The amount of dispersant necessary to form a high solids loading slurry is relatively large. Concentrations near 4 wt% to powder weight were necessary to form a fluid slurry of high solids content.

Often, colloidal stability is characterized by the value of zeta potential. For dispersions of nanopowders, the counterion concentration generated by the surface area and the amount of dispersant added generates significant salt levels. Conductivity was used to characterize the electrolyte level in the PMA dispersed suspensions. Figure 4(a) plots the measured particle zeta potential as a function of the volume fraction of solids, and conductivity of the suspensions is also plotted for reference. Figure 4(b) shows the zeta potential at a constant solids loading of 4.73 vol% as the conductivity is increased by the addition of KNO_3 electrolyte solution. By comparison of the two graphs, it is clear that increasing solids content by itself does not raise the salt level beyond 0.35. At low volume fraction, this does not reduce the zeta potential by a significant amount, but for the samples at high-volume solids, the zeta potential is significantly reduced. Clearly, the reduction in zeta potential is not caused by increased monovalent electrolyte concentration alone.

The decreasing strength of the zeta potential directly impacts the flow properties of the suspensions. The effects of solids loading are shown by the rheology characterization measurements, given in Fig. 5. The figure shows the slurry viscosity at 750 s^{-1} and a least squares fit of the modified Krieger–Doughtery equation. The parameters of this equation are commonly used to characterize the maximum packing fraction of the slurry in the linear viscosity region, and a particle shape parameter. For the PMA dispersed suspension, $\phi_m = 0.582$, and $[\eta] = 5.3$. The shape factor of the equation is reasonable in comparison with the morphologies shown in Fig. 3 as the larger particle fractions are slightly non-equiaxed and show some grain boundaries, but does not forbid the presence some small aggregates or particle doublets.

Although the modeling of the shear rate data suggests that a maximum solids loading approaching 58% solids can be achieved, our experience with this powder showed that a hard-packed body is formed at volume fractions solids of near 43–46%. In Fig. 6, the oscillatory characteristics of the PMA dispersed suspension under a shear stress sweep at 1 Hz are presented. As volume fraction is increased, the elastic modulus G′ becomes increasingly strong and constant over the stress range investigated, and the viscoelastic component G″ is stronger at low volume fraction, but weaker above a transition near 38 vol%. Clearly, the PMA dispersed particles are developing elastic characteristics at unexpectedly low volume fractions. As zeta potential values are decreasing with volume fraction, the elastic properties are likely developed as a result of weak attraction forces between particles or the development of a weak interparticle network similar to a particle gel.

The unusual phenomenon in this system is the reduction in zeta potential strength as solids loading is increased. The zeta potential of the dispersed material is controlled by the adsorbed polyelectrolyte, and the interactions of the solution components with the polyelectrolyte will dictate its effectiveness as a dispersant. The tests in Fig. 4(b) showed that counter-ions do screen the electrostatic charge of the dispersant layer to lower the measured zeta potential, but the effect is much stronger as volume fraction is increased than can be explained by the conductivity of the solution. Solids fraction effects were previously considered to reduce zeta potential by Johnson et al.,[12] who applied an empirical correction. However, the instrument used in our studies uses a complete theory that requires no volume fraction correction, and therefore the zeta potential reduction is real.[13–15] An additional factor in this material is the large number of

dopants, which exhibit varying degrees of solubility and valence in solution.

The interaction between polyelectrolyte adsorbed layers and plurivalent counter-ions affect the adsorbed amount and conformation of the layer in addition to having stronger electrostatic screening effects.[16,17] Abraham et al. have shown that force curves between anionic polyelectrolytes are sensitive to the addition of divalent cations.[18] All divalent cations screen the forces between the polyelectrolyte chains, and specific adsorption of the cations to the solid surface can eliminate negative charged sites on the substrate and promote higher adsorbed amounts. From the speciation chemistry investigated for the particle solubility versus pH, the only positively charged species in this system at pH 9.1 are Zn^{2+} ions, and the dispersion pH is very close to the onset of very high zinc solubility. The relatively high concentration of dispersant necessary for slurry formation suggests that zinc dissolution is affecting the polyelectrolyte adsorption. Abraham et al. found that the incorporation of Ca^{2+} ions with poly (acrylic acid) adsorbed brushes created a complex profile of long-range stabilization, an attractive short-range regime at intermediate separation, and a short-range repulsive interaction at close separations. The attractive intermediate regime was attributed to divalent ion–induced bridging between layers in their study. We have performed all processing as close to the minimum in solubility as possible, but there is no guarantee that some dissolution does not occur during attrition milling. In fact, increased solubility of zinc ions during milling would promote the relatively high concentration of dispersant found necessary to disperse this powder.

Ammonium polymethacrylate is known to form chemical complexes with Zn^{2+}, and the binding energy of Zn^{2+} is stronger than that of Ca^{2+}.[16] The adsorption of divalent cations can be represented according to the apparent equilibrium constant for the complexation reaction, with the assumption that the bound Zn^{2+} ions form a dimeric complex

$$k_{app} = k_1 \exp(-2e_0 \Psi_p/kT) = \frac{[Zn^{2+}]_{bound}}{[Zn^{2+}][-COO^-]^2} \quad . \quad (2)$$

If the zinc concentration is raised in the solution, the complexation reaction will be promoted to achieve chemical equilibrium. If $[Zn^{2+}]$ is decreased in the solution, bound Zn^{2+} in the dispersant layer would be likewise released. This process would affect the particle zeta potential in accord with our observations. As solvent is removed to concentrate the solids loading, any dissolved zinc ions in solution become more concentrated and reduce the value of the measured zeta potential. At some critical complex concentration, the value of the particle zeta potential would be insufficient for dispersion of the particles, and a particle gel would form. This gel might involve binding between dispersant layers on adjacent particles as well.

Although this hypothesis appears to incorporate all our observations, we cannot claim that it is the definitive phenomenon causing the instability of the particles in this dispersion. A more focused study is required to answer this question completely.

Addition of PEG400 plasticizer

The PMA dispersed suspension with 10 wt% PEG400 has modified Kreiger–Doughtery equation parameters of $\phi_m = 0.63$ and $[\eta] = 4.84$. Figure 4 shows that the zeta potential is more resistant to increases in volume fraction of solids when PEG400 is present in the solution phase. The effect of monovalent electrolyte seems to converge in the suspensions tested. In Fig. 5, the data indicates that the addition of PEG400 reduces the high shear viscosity of the suspensions and raises the maximum solids loading. Oscillatory measurements were also conducted for these suspensions, but the elastic components were largely below detection limits for the instrument below the highest volume fraction. These equation parameters suggest that the particle morphologies are more equiaxed after its addition, but the values remain similar to the observed particle morphologies. The lowering of the shape factor and increase of the maximum packing fraction suggests that PEG400 is increasing particle stability and inhibiting the formation of flocculated particles at high solids loading.

The action of PEG400 to improve the stability of the particles at high solids loading suggests that it interacts within the dispersant layer to prevent the hypothesis of divalent ion binding. Solutions of poly ethylene oxide and polymethacrylate have been extensively studied for their hydrogen bonding interactions, and it is accepted that the polymers do have an interaction leading to precipitation, although this is only seen at very low degrees of ionization of the polymethacrylate.[19] In the case of polymer layers, the argument of low degree of ionization appears modified.[20–22] Netz showed that the dielectric constant of the interface affects the dissociation reaction of an adsorbed polyelectrolyte.[22] Podhajecka et al. found that the degree of polyelectrolyte dissociation near the interface does not correspond to the bulk pH, and that the polyethylene oxide segregated to the nonpolar interface to form an interpolymer complex that resists bulk conditions very strongly.[20] Based on these studies, it is plausible that PEG400 acts as a very low molecular weight polyethylene oxide polymer and intercalates within the inner layers of the polymethacrylate dispersant to provide a stronger steric repulsion between particles.

Therefore, the argument is strong that multivalent ion complexes forming within the dispersant layers of the

particles explain the behavior seen in this powder. As solids loading increases, ion binding is proposed to reduce the zeta potential. As colloidal stability decreases, the flocculated structures are formed that raise viscosity and prevent the attainment of high solids loading. The addition of PEG400 inhibits the formation of this attractive force through intercalation within the dispersant layer and increased repulsion. This delays the formation of flocculated structures and allows for the achievement of higher solids loadings with fluid response.

V. CONCLUSIONS

A chemically prepared, doped zinc oxide powder was characterized and processed for near-net-shape forming methods of colloidal processing. The minimum in component solubility was found in aqueous solution at pH 9.1. The initial material was aggregated, and attrition milling with ammonium polymethacrylate was largely successful in breaking down the aggregates into primary particles. The primary particles exhibit a trimodal distribution, in which the largest fraction is composed of the remaining hard aggregates. Suspensions of these materials exhibited a viscoelastic to elastic behavioral transition at relatively low volume concentrations between the range 30–40 vol% solids. The mechanism for this transition involved a reduction in the zeta potential of the dispersed particles and is proposed to relate to chemical complexation of zinc ions within the dispersant layers. As solids loading increases, zinc ions are concentrated in the solution, which promotes the binding interaction and reduces zeta potential. The addition of polyethylene oxide 400 to the solution phase greatly reduced the elastic component of the particle suspensions for the evaluated solids loading. The reduction of the attractive interaction between particles is proposed to relate to intercalation of the polyethylene oxide within the ammonium polymethacrylate layers to inhibit ion binding between particles. This allows for the attainment of higher solids loading in suspension.

REFERENCES

1. W.M. Sigmund, N.S. Bell, and L. Bergstrom, Novel powder processing methods for advanced ceramics, *J. Am. Ceram. Soc.* **83,** 1557 (2000).
2. A. Vojta and D.R. Clarke, Electrical-impulse-induced fracture of zinc oxide varistor ceramics, *J. Am. Ceram. Soc.* **80,** 2086 (1997).
3. R.G. Dosch, B.A. Tuttle, and R.A. Brooks, Chemical preparation and properties of high-field zinc oxide, *J. Mater. Res.* **1,** 90 (1986).
4. T.J. Gardner and S.J. Lockwood, Scale-up of a batch-type chemical powder preparation process for high field varistor fabrication, Sandia Report, SAND87-2194, Feb. 1988.
5. K.M. Kimball and D.H. Doughty, Aluminum doping studies on high field ZnO varistors, Sandia Report, SAND86-0713, Aug. 1987.
6. T.J. Gardner, D.H. Doughty, S.J. Lockwood, B.A. Tuttle, and J.A. Voigt, The effect of low level dopants on chemically prepared varistor materials, *Ceramic Transactions* (American Ceramic Society, Inc., Westerville, OH, 1989), 3.
7. L. Bergstrom, K. Shinosaki, H. Tomiyama, and N. Mitzutani, Colloidal processing of a very fine $BaTiO_3$ powder—effect of particle interactions on the suspension properties, consolidation, and sintering behavior, *J. Am. Ceram. Soc.* **80,** 291 (1997).
8. L. Bergstrom, Rheological properties of concentrated, nonaqueous silicon nitride suspensions, *J. Am. Ceram. Soc.* **79,** 3033 (1996).
9. J. Cesarano, I.A. Aksay, and A. Bleier, Stability of aqueous alpha-alumina suspensions stabilized with polyelectrolytes, *J. Am. Ceram. Soc.* **71,** 250 (1988).
10. J. Cesarano and I.A. Aksay, Processing of highly concentrated aqueous alpha-alumina suspensions with poly(methacrylic acid) polyelectrolyte, *J. Am. Ceram. Soc.* **71,** 1062 (1988).
11. C.F. Baes and R.E. Mesmer, *The Hydrolysis of Cations* (Krieger Publishing Co., Malabar, FL, 1986).
12. S.B. Johnson, A.S. Russell, and P.J. Scales, Volume fraction effects in shear rheology and electroacoustic studies of concentrated alumina and kaolin suspensions, *Colloids Surf. A* **141,** 119 (1998).
13. A.S. Dukhin and P.J. Goetz, Acoustic and electroacoustic spectroscopy for characterizing concentrated dispersions and emulsions, *Adv. Colloid Interface Sci.* **92,** 73 (2001).
14. A.S. Dukhin and P.J. Goetz, New developments in acoustic and electroacoustic spectroscopy for characterizing concentrated dispersions, *Colloids Surf. A* **192,** 267 (2001).
15. Andrei Dukhin, personal communication.
16. R.D. Porasso, J.C. Benegas, and M.A.G.T. van den Hoop, Chemical and electrostatic association of various metal ions by poly(acrylic acid) and poly(methacrylic acid) as studied by potentiometry, *J. Phys. Chem. B* **103,** 2361 (1999).
17. J. Sun, L. Bergstrom, and L. Gao, Effect of magnesium ions on the adsorption of poly(acrylic acid) onto alumina, *J. Am. Ceram. Soc.* **84**, 2710 (2001).
18. T. Abraham, A. Kumpulainen, Z. Xu, M. Rutland, P.M. Claesson, and J. Masliyah, Polyelectrolyte-mediated interaction between similarly charged surfaces: Role of divalent counter ions in tuning surface forces, *Langmuir* **17,** 8321 (2001).
19. M. Zeghal and L. Auvray, Structure of polymer complexes in water, *Europhys. Lett.* **45,** 482 (1999).
20. K. Podhajecka, M. Stepanek, K. Prochazka, and W. Brown, Hybrid polymeric micelles with hydrophobic cores and mixed polyelectrolyte/nonelectrolyte shells in aqueous media. 2. Studies of the shell behavior, *Langmuir* **17,** 4245 (2001).
21. H.H. Rmaile and J.B. Schlenoff, Internal *p*Ka's' in polyelectrolyte multilayers: Coupling protons and salt, *Langmuir* **18** (2002).
22. R.R. Netz, Charge regulation of weak polyelectrolytes at the low- and high-dielectric constant substrates, *J. Phys. Condens. Matter* **15,** S239 (2003).